

EXOSAT OBSERVATIONS OF THE X-RAY BINARY PULSAR 4U 1538–52

N. R. ROBBA¹

Istituto di Fisica, Università degli Studi di Palermo

G. CUSUMANO²

Istituto di Fisica Cosmica ed Applicazioni dell'Informatica, Consiglio Nazionale delle Ricerche, Palermo

M. ORLANDINI³

Scuola Internazionale Superiore di Studi Avanzati, Trieste

D. DAL FIUME⁴

Istituto di Studio e Tecnologie delle Radiazioni Extraterrestri, Consiglio Nazionale delle Ricerche, Bologna

AND

F. FRONTERA⁴

Istituto di Studio e Tecnologie delle Radiazioni Extraterrestri, Consiglio Nazionale delle Ricerche, Bologna; and Dipartimento di Fisica, Università degli Studi di Ferrara

Received 1991 February 14; accepted 1992 June 6

ABSTRACT

The Medium Energy experiment on-board the *EXOSAT* satellite observed the X-ray binary system 4U 1538–52 on four occasions during 1984 March and August. Observed pulsation periods of 529.97 ± 0.16 s (March 17) and 530.14 ± 0.03 s (August 10) indicate that the neutron star in the 4U 1538–52 system continued to spin down with $\dot{P}_p = +3.9 \times 10^{-9}$ s s⁻¹ ($\dot{P}_p/P_p = +2.3 \times 10^{-4}$ yr⁻¹) in the time period of 1976–1988. In the first observation an absorbing episode was observed, which may be attributed to an inhomogeneity in the stellar wind of QV Nor; the scale height of this blob is 2×10^9 – 2×10^{10} cm, assuming a blob velocity of 100–1000 km s⁻¹, of the same kind of inhomogeneities observed in the Vela X-1 system. Using the eclipse transition time of ~ 0.06 days we can confirm the scale height of $\sim 1.5 \times 10^{11}$ cm for the atmosphere of the optical counterpart. The source shows prominent aperiodic time variability: the frequency spectra for the two observations out of eclipse are well fitted by a power law ($kf^{-\alpha}$) plus a constant, with slope $\alpha_t = 1.63 \pm 0.09$ and $\alpha_t = 1.73 \pm 0.07$ for the March 17 and August 10 observations, respectively. The rms's are in agreement with those observed in other high-mass X-ray pulsars: $26 \pm 5\%$ for the March observation and $36 \pm 6\%$ for the August observation. The 1.5–12 keV phase-averaged X-ray spectrum is consistent with a power law of photon spectral index of 1.49 ± 0.04 (March 17) and 1.4 ± 0.07 (August 10), and shows an iron line with an EW of ~ 100 eV. The energy spectra show variations with pulse phase. A detailed study of these variations with pulse phase is discussed.

Subject headings: binaries: close — pulsars: individual (4U 1538–52) — X-rays: stars

1. INTRODUCTION

The X-ray source 4U 1538–52 (Forman et al. 1978) belongs to that particular class of objects which show a pulsed emission when observed in the X-ray energy band. It is a binary system formed by a 14.5 mag B0 supergiant, QV Nor (Cowley et al. 1977; Apparao et al. 1978; Schwartz et al. 1978), and a neutron star which spins with a period of ~ 530 s (Davison 1977; Becker et al. 1977). The X-ray luminosity of 4U 1538–52, assuming a distance of 6 kpc (Parkes et al. 1978; Crampton, Hutchings, & Cowley 1978), is $\sim 2 \times 10^{36}$ ergs s⁻¹. This system also exhibits a 0.51 day long X-ray eclipse, with an orbital period of ~ 3.73 days, and a projected X-ray source semimajor axis of 55 lt-sec (Becker et al. 1977; Crampton et al. 1978; Davison et al. 1977; Makishima et al. 1987, hereafter MKHN). From these values it is not possible to distinguish

whether QV Nor fills or slightly underfills its Roche lobe, and therefore if 4U 1538–52 is a wind-fed or a disk-fed binary system. However, as argued by MKHN, the lack of a secular spin-up trend can be taken as a suggestion that 4U 1538–52 is not a disk-fed system. From the value of the typical mass-loss rate from a supergiant as QV Nor, of the order of $10^{-6} M_\odot$ yr⁻¹, one can infer only that the wind activity is of great importance in the process of mass transfer from the primary to the neutron star.

The pulse-phase averaged X-ray spectrum of 4U 1538–52 has been well fitted by the canonical model for X-ray pulsars, namely a power-law continuum modified by a high-energy cutoff. A problem of contamination by the galactic ridge emission, as pointed out by MKHN, may exist. An iron K α emission line at 6.3 keV with an EW of ~ 50 eV has also been detected by MKHN and with an EW of ~ 570 eV by White, Swank, & Holt (1983). Recently, a cyclotron line feature at ~ 20 keV has been detected by the *Ginga* satellite observatory (Clark et al. 1990).

In this paper we report results from a temporal and spectral analysis performed on four *EXOSAT* observations, part of which were taken from the *EXOSAT* archival, carried out during 1984 March and August.

¹ Postal address: Dipartimento di Fisica, via Archirafi, 36, I-90123, Palermo, Italy.

² Postal address: IFCAI/CNR, via Mariano Stabile, 172, I-90139, Palermo, Italy.

³ Postal address: Scuola Internazionale Superiore di Studi Avanzati, via Beirut 2, I-34014, Trieste, Italy.

⁴ Postal address: Istituto TESRE/CNR, via de' Castagnoli, 1, I-40126 Bologna, Italy.

2. OBSERVATIONS AND ANALYSIS

The X-ray satellite *EXOSAT* observed 4U 1538–52 on four occasions on 1984 March 17 and August 7, 10, and 11. Details for each observation are given in Table 1.

The present analysis is based on data from the argon cells of the Medium Energy proportional counter (ME). The ME detector was operated with two quadrants offset to provide a background monitor and the other two quadrants aligned pointing the source. Counts were accumulated into energy histograms of 255 channels for each of the eight ME argon and xenon counters with an integration time of 10 s. In parallel various high time resolution modes were running. Background measurements during the slew maneuver preceding and following the observations were also available. A complete description of the *EXOSAT* mission and scientific instruments can be found in Taylor et al. (1981); de Korte et al. (1981); Turner, Smith, & Zimmermann (1981); and White & Peacock (1988).

TABLE 1
JOURNAL OF OBSERVATIONS

Observation Number	Date (1984)	Start Time (U.T.)	Duration (s)	Binary Phase ^a	Half ME on Source
1	Mar 17	09 ^h 36 ^m	35,400	0.40–0.51	H2
2	Aug 7	20 03	16,400	0.87–0.92	H2
3	Aug 10	02 48	22,500	0.48–0.54	H1
4	Aug 11	12 53	25,000	0.86–0.93	H2

^a Ephemeris were taken from MKHN.

In each observation the source was always pointed by one half detector while the other half detector monitored the background. The background subtraction was made as follows: first, a difference between the background in the two halves of the detector was computed using data obtained during the slew maneuver; then, the background to be subtracted was evalu-

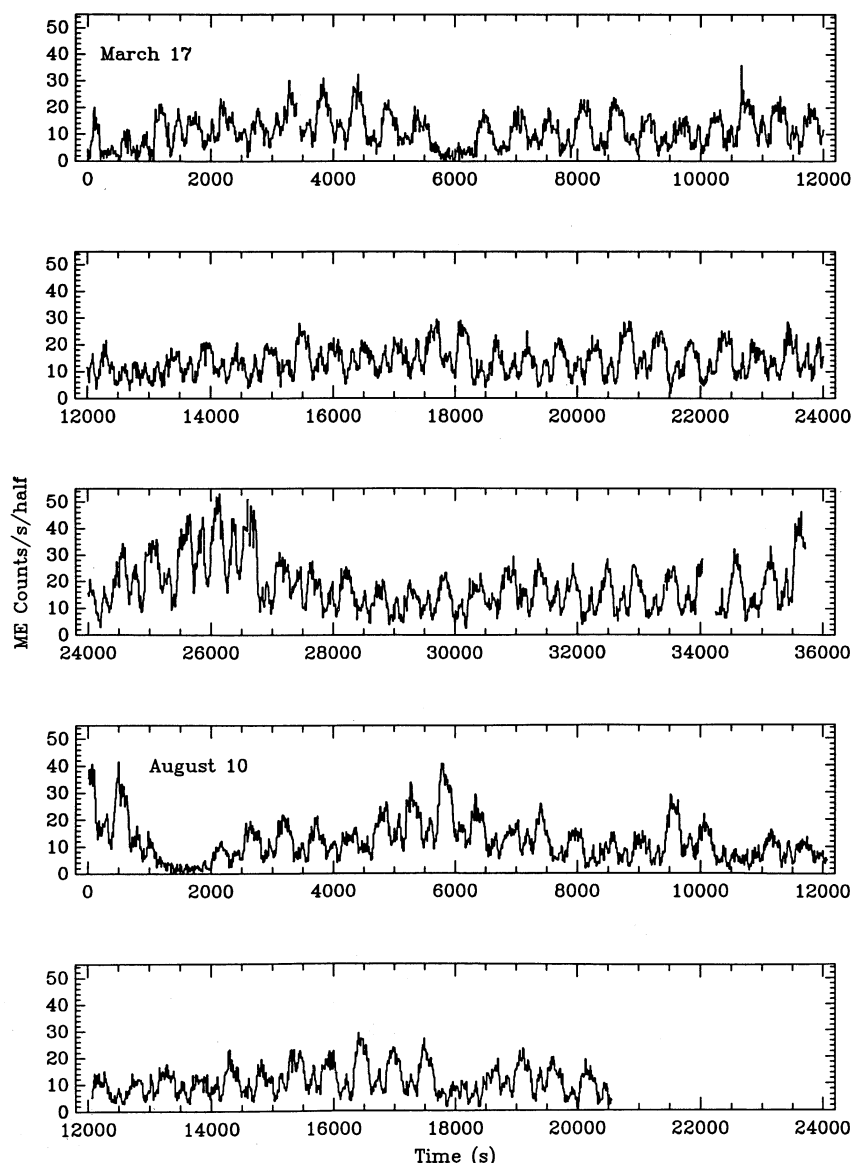


FIG. 1.—The 1–11 keV background subtracted light curves of 4U 1538–52 of 1984 March 17 and August 10 observations

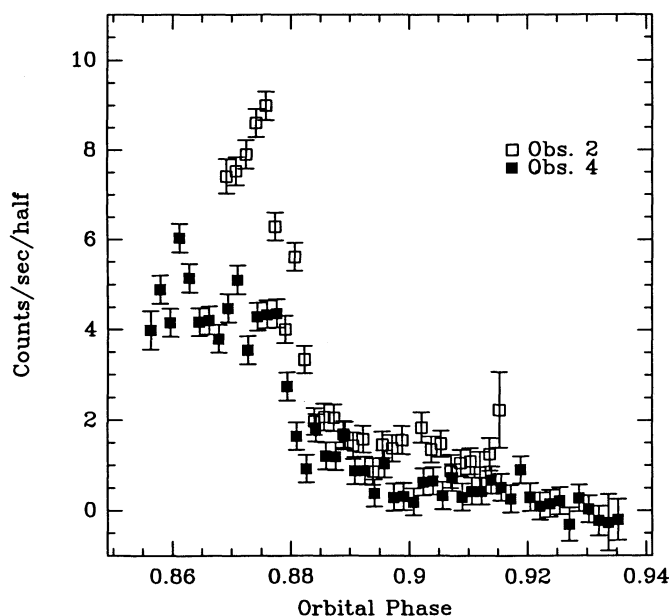


FIG. 2.—The 1–11 keV background subtracted light curves of 4U 1538–52 during its eclipse ingress. Open squares: August 7 observation; filled squares: August 11 observation. Orbital ephemeris are taken from MKHN.

ated correcting by this difference the background measured by the offset half detector during the observation of the source.

The 1–11 keV background subtracted light curves of the March 17 and the August 10 observations are shown in Figure 1, with 10 s time resolution. In the first one we can distinguish an episode of increasing luminosity ~ 2000 s long starting 24,000 s from the beginning of the observation, while an intensity dip ~ 1000 s long is present at the beginning of the August 10 observation.

The intensity is highly variable, ranging from ~ 50 counts s^{-1} half $^{-1}$ during the flare to ~ 1 counts s^{-1} half $^{-1}$ during the dip, with a mean value of ~ 16 and ~ 14 counts s^{-1} half $^{-1}$ in the two observations, respectively. The background-subtracted X-ray light curves versus binary phase were derived by folding the data with the orbital parameters given by MKHN. The light curves obtained during the August 7 and August 11 observations in the 1–11 keV energy range, are shown in Figure 2 with 530 s time resolution. A gradual entry into

eclipse of the X-ray source, with a transition time of ~ 5000 s, is clearly visible in both observations. This time, consistent with the value reported by MKHN, gives a scale height of $\sim 1.5 \times 10^{11}$ cm for the atmosphere of QV Nor using the orbital parameters given by MKHN.

2.1. Timing Analysis

In the first and third observations (see Table 1) the single 530 s X-ray pulses from 4U 1538–52 were well visible (see Fig. 1). We have determined the arrival times of each individual pulse as follows: we assumed the pulse minima as a fiducial point, and we measured its arrival time, after smoothing the data to reduce the effect of random fluctuations. The pulse arrival times were corrected to the solar system barycenter and for the orbital motion of the X-ray source using the ephemerides obtained by MKHN. A least-squares analysis was used to determine the best-fitting constant pulse period.

In the other two observations the single pulses were not visible. We considered the part of observation in which the source was not in eclipse and subdivided it into intervals of length 2000–5000 s, and we folded the data with the previously obtained period. Using the above procedure we determined the arrival times of these pulses. A least-squares analysis was then used again.

For the first observation the timing residuals were minimized for a period of 529.97 ± 0.16 s and a rms timing residual of 18 s. For the third plus the available data from the second and fourth observations, the timing residuals were minimized for a period of 530.14 ± 0.03 s with a rms timing residual of 15 s.

The results of this analysis are shown in Figure 3 together with previous determinations. Our new values, together with values from *OSO 8* (Becker et al. 1977), *Ariel 5* (Davison 1977; Davison et al. 1977), *Tenma* (MKHN), and *Ginga* (Nagase 1989), indicate that 4U 1538–52 was steadily spinning down during 1983–1984 with $\dot{P}_p/P_p \sim 1.9 \times 10^{-11} s^{-1}$. The general trend in the period 1976–1988 is a spin-down with $\dot{P}_p/P_p \sim 7.3 \times 10^{-12} s^{-1}$ (dashed line in Fig. 3).

2.2. Aperiodic Variability

In the study of the temporal behavior of 4U 1538–52 we investigated the aperiodic variability, in order to obtain information about the time scales of the intensity variations which are not associated to the pulsation. Our main tool to investi-

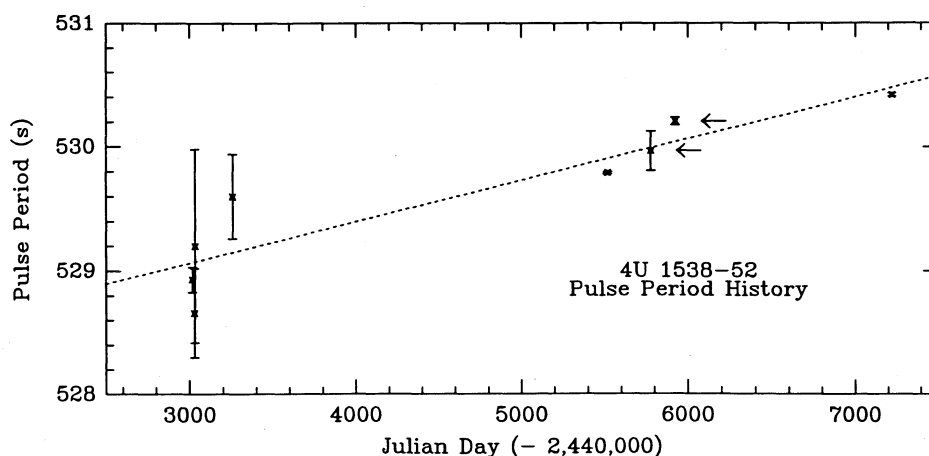


FIG. 3.—Pulse period history of 4U 1538–52. Our measurements are indicated by arrows.

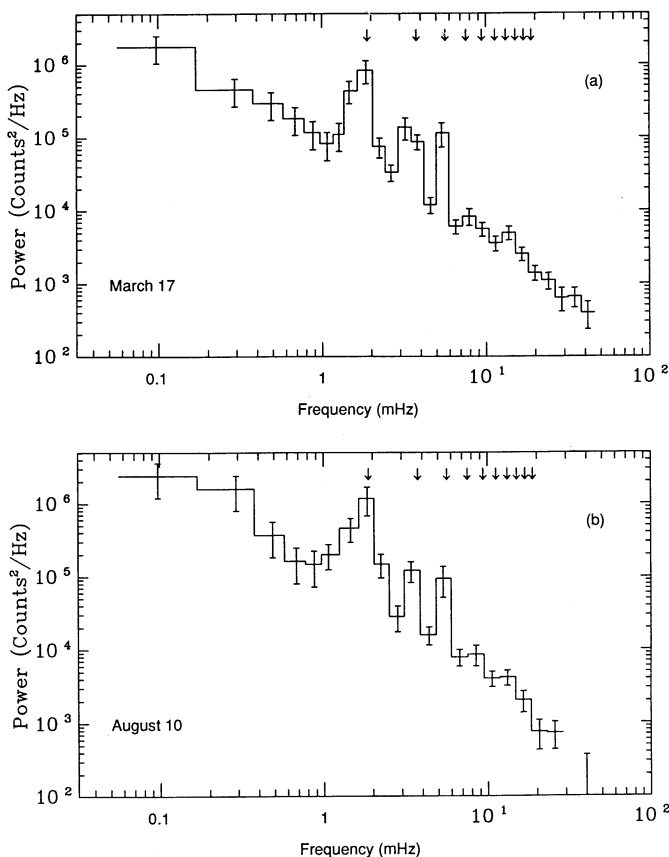


FIG. 4.—Estimates of the power spectral density of the X-ray intensity of 4U 1538–52. The Nyquist frequency is 50 mHz. The fundamental frequency of pulsation, and its first nine harmonics are indicated by arrows.

gate this variability is the estimate of the power spectral density (PSD) via Fast Fourier Transform (FFT). We studied the PSDs of the count rate of 4U 1538–52 for both the first and third observations. For both observations we used count rates obtained from the spectral data with 10 s time resolution. In addition, for the third observation, count rates with 16 ms time resolution in one energy band (1.2–6.1 keV) were available.

For the spectral data, the 1–8 keV energy band was chosen to have an optimal signal-to-noise ratio. We performed our analysis by dividing the first observation into six runs and the third observation into four runs containing 512 data points each. We computed the PSD for each run. Then for each observation we obtained the average PSD. For both the observations the results are shown in Figure 4a and 4b, where the white noise level was subtracted (see below). The PSD function so obtained gives the frequency dependence of the variance of the data due to aperiodic variations in the flux of the source. The peaks visible in the plots correspond to the fundamental frequency of pulsation and to some of its harmonics: the fundamental frequency and all the detected harmonics are indicated by arrows in Figure 4a and 4b. These figures show that the source has aperiodic time variability with time scales down to the Nyquist frequency of 0.05 Hz.

In order to investigate the continuum component of our spectra the first step was to evaluate the contribution due to the pulsation. We considered a general power spectrum of a

TABLE 2
FITTING RESULTS ON POWER SPECTRA

Observation Number	Resolution Time (s)	$\langle I \rangle$ (counts s $^{-1}$)	α_t	Root Mean Square (%)	χ^2_{dof}
1	10	16.82 ± 0.04	1.63 ± 0.09	26 ± 5	8/12
3	10	14.09 ± 0.04	1.73 ± 0.07	36 ± 6	9/15

pulsed source as the sum of three terms:

$$P(f) = \underbrace{C}_{\text{Poissonian}} + \underbrace{kf^{-\alpha_t}}_{\text{aperiodic}} + \underbrace{\sum_n A_n \delta(f - nf_p)}_{\text{coherent}}, \quad (1)$$

where k , α_t , and C (the Poissonian counting) are three constants, f is the frequency, $f_p = 1/P_p$ and A_n are the amplitudes of the fundamental and its harmonics. In fitting the power spectrum given by equation (1) to the measured PSDs we also took into account the effect due to the leakage of power from the peaks due to the pulsation (see, e.g., Angelini, Stella, & Parmar 1989). The amplitudes A_n of the peaks were estimated from the original (not rebinned) PSDs and they were considered as fixed parameters in the fitting procedure. We performed a fit to the measured power spectra binned logarithmically, with free parameters k , α_t , and C . The values of α_t obtained from these fits are shown in Table 2. The same analysis was performed on the data taken from the third observation with 16 ms time resolution. The result is shown in Figure 5: no power is apparent above 0.05 Hz. We computed the rms fractional variability of the continuum component following Lewin, van Paradijs, & van der Klis (1988). The results are shown in Table 2. They are in agreement with those obtained for other massive X-ray pulsars (Belloni & Hasinger 1990).

2.3. Pulse-Phase Averaged Spectrum

The energy spectral analysis has been performed using only the data obtained from argon ME detectors in the energy

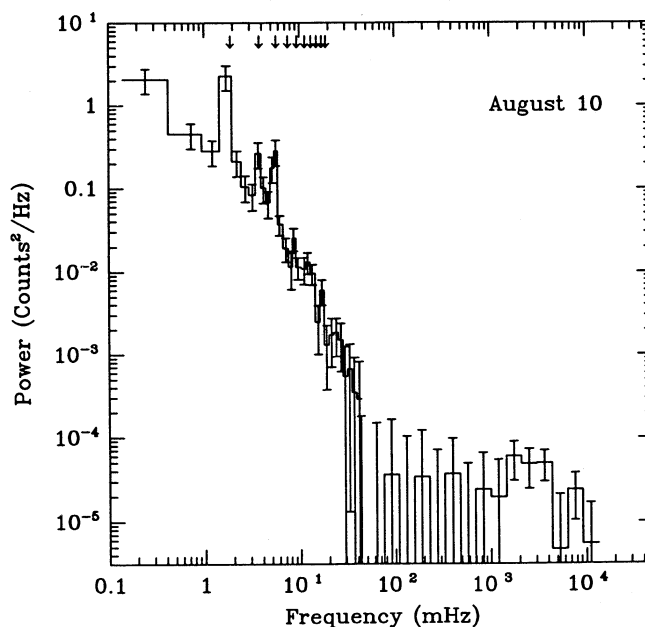


FIG. 5.—Estimate of the power spectral density of the X-ray intensity of 4U 1538–52 using data with 16 ms time resolution.

range 1.5–12 keV. In previous observations, the X-ray spectrum of 4U 1538-52 was fitted by a power law plus a low-energy absorption and a high-energy cutoff (see, e.g., Nagase 1989). Given the limited energy range of our spectral analysis, we used as spectral laws a thermal bremsstrahlung model and a power law, both of them with low-energy photoelectric absorption. Both a power law and a thin thermal bremsstrahlung law fit well to the data. In Table 3, we show the results of the power-law fits for the first and the third observations. The energy spectra appear to be slightly steeper than those measured by MKHN. An iron line at a fixed energy of 6.7 keV with an EW \approx 100 eV is consistent with our data, but the insertion of such a line does not improve significantly the χ^2 . Incidentally we note that these values are in agreement with the *Tenma* measurement (MKHN), but a factor 5 smaller than the *HEAO 1-A2* measurement (White, Swank, & Holt 1983). As pointed out by MKHN, this discrepancy is probably due to a contamination from the Galactic ridge, whose emission is strong in the direction of 4U 1538-52 (Warwick et al. 1985; Koyama 1989). We expect that our results are not affected by systematic errors. Indeed the field of view of the ME detectors (45' FWHM) gives a solid angle at least 10 times smaller than that of the *Tenma* detectors. Thus we expect a negligible contamination from the galactic ridge. Moreover our background subtraction procedure uses a background estimate from the offset detectors, which also are pointing to the galactic ridge.

The hardness ratio $R = F(4-10 \text{ keV})/F(1-4 \text{ keV})$ for the first and the third observation, as a function of time is shown in the

TABLE 3
EXOSAT SPECTRAL MEASUREMENTS OF 4U 1538-52^a

Observation Number	Photon Index	N_H ($10^{22} \text{ H cm}^{-2}$)	Flux ^b	χ^2_{dof}
1	1.25 ± 0.03	1.65 ± 0.13	3.0	1.12
3	1.40 ± 0.05	2.69 ± 0.25	2.2	1.34
1 (hard)	1.32 ± 0.12	3.59 ± 0.64	2.3	0.83

^a 1 σ error.

^b Units of $10^{-10} \text{ ergs s}^{-1} \text{ cm}^{-2}$.

bottom panels of Figure 6a and 6b. There is no appreciable change of hardness ratio during the flare observed in the first observation, confirming the general rule for X-ray pulsars that the hardness ratio does not depend on intensity. During the observation of day 84/223 a spectral softening is apparent at the beginning of the observation, in correspondence of a very low flux level. Very likely this softening is due to small systematic errors in the background subtraction. However, an episode of significant variation of hardness ratio at approximately constant intensity is present in the first observation. This event may be due to an inhomogeneity in the stellar wind of QV Nor, which passed through our line of sight and caused the observed absorption in the 1–4 keV energy band. The scale height of this inhomogeneity, assuming a blob velocity of the order of 100–1000 km s^{-1} , is 2×10^9 – $2 \times 10^{10} \text{ cm}$. This is in agreement with the observation of inhomogeneities in the

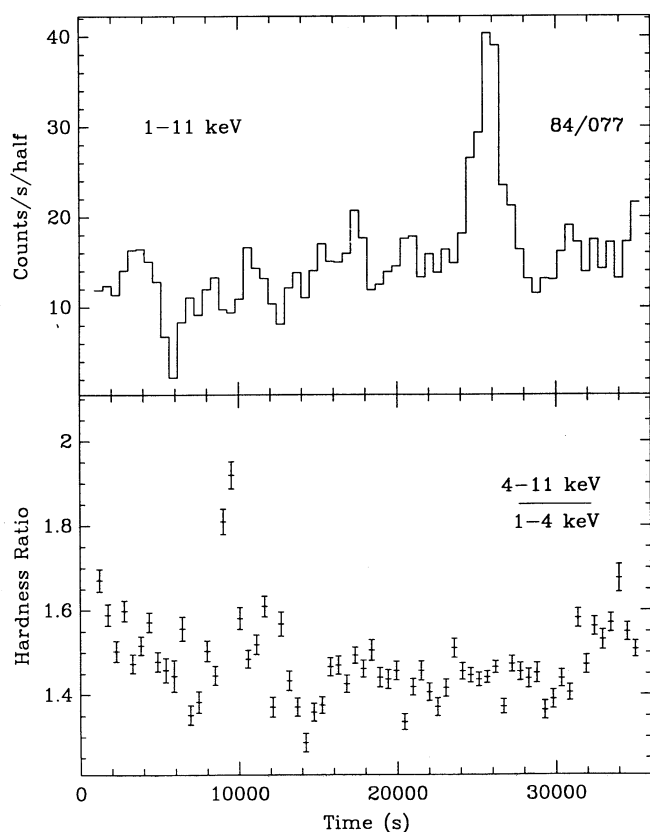


FIG. 6a

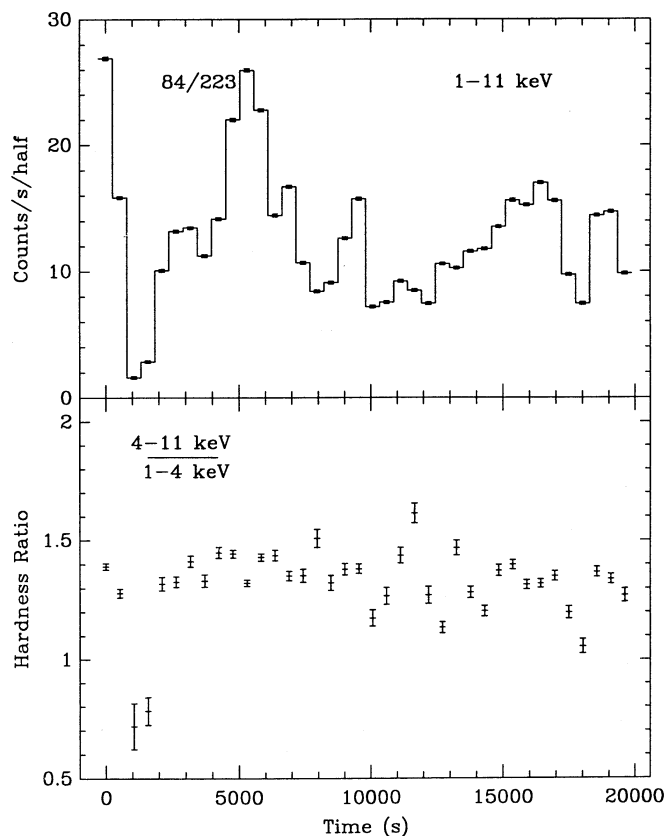


FIG. 6b

FIG. 6.—Top panels: 1–11 keV count rate from 4U 1538-52 with 530 s integration time. Bottom panels: hardness ratio (4–11 keV)/(1–4 keV). (a) Observation of 1984 March 17; (b) observation of 1984 August 10. The statistical errors in the top panel are of the order of the thickness of the line of the plot.

wind-fed X-ray pulsar Vela X-1 reported by Nagase et al. (1986). To analyze what type of spectral variation occurred in this episode, we compared the average spectrum obtained integrating during the period with high hardness ratio with other spectra obtained outside the episode. The spectral ratio in Figure 7 shows remarkable variations in the 1–3 keV and 6–7 keV energy bands. The attenuation of the flux in the low-energy band is typical of an increased absorption. The attenuation of the intensity close to the iron line is more surprising, taking also into account that the ratio above and below the line is fairly constant. We can infer directly from this variability that this line is really emitted from 4U 1538–52, and it is not a contamination from the galactic ridge, since we do not expect a time variability of this contamination. The comparison among various spectra taken outside this episode do not show any feature in their ratios: all of them are statistically consistent with each other, i.e., their ratios are constant with energy.

We performed a fit to the source spectrum obtained during this episode. The results are reported in Table 3. It is evident that the slope of the power law is still consistent with the slope measured for the average spectrum of the entire observation, while the N_H value clearly changed.

2.4. Pulse-Phase Spectroscopy

The time-averaged background subtracted pulse profiles in different energy bands, obtained by folding the data at the pulse period, are shown in Figures 8 and 9 for the first and the third observation, respectively. The counts have been normalized to the average count rate in each light curve. They show a double-peak structure with the first peak brighter than the second one, separated by two minima of about the same intensity. The pulse profiles depend on energy, and a dip is present in the 1–3 keV light curve at the maximum of intensity. This feature was also observed by *Ginga* (Clark et al. 1990). At high energies the main pulse is sharper, while the interpulse becomes broader.

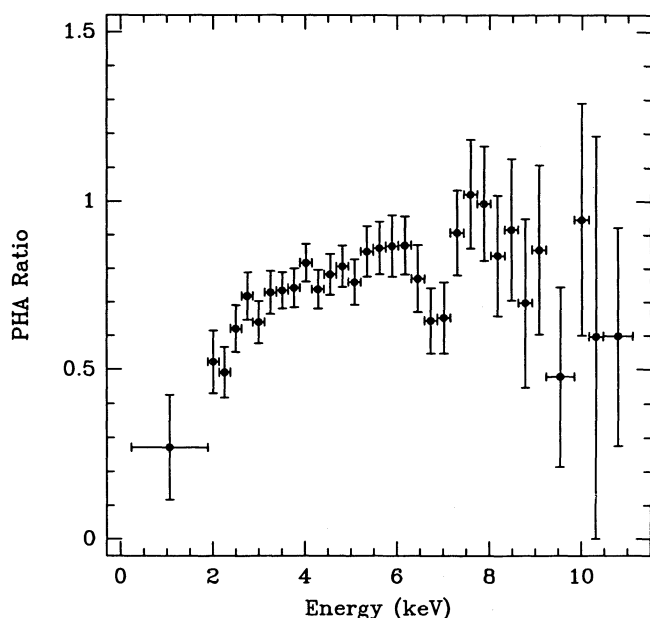


FIG. 7.—Ratio between count-rate spectra obtained during and outside the episode of increased absorption.

We folded the same data in the energy intervals 1–4 keV and 4–11 keV and computed the corresponding hardness ratio. The result together with the pulse profile obtained folding the data in the 1–11 keV energy range is shown in Figure 10. This hardness ratio shows a very complex behavior with pulse phase, reminiscent of those observed from other X-ray pulsars (A0 535+26, GX 1+4, etc.).

We performed a pulse-phase resolved spectroscopy, by dividing the light curve in 10 broad intervals each 0.1 wide in pulse phase. For each interval we obtained a source spectrum, and we fitted each spectrum with a power law plus low-energy absorption model. We also used in our fits a power law plus iron emission-line model, with no significant improvement of χ^2_{dof} . The results from the fits with a power law are reported in Figure 10. To allow a direct comparison of the results from our observations and from the observation of *Ginga* (Clark et al. 1990), the pulse phase is tentatively aligned to pulse phase 0 of the observation of *Ginga*. This alignment is only based on the shape of the three measured pulse light curves.

As the August 10 observation was performed with the source at a lower flux level ($\sim 20\%$ less than in March 17) and for a shorter time, the results of the pulse-phase spectroscopy have a lower statistical quality. As can be seen the spectrum is harder at phase ~ 0 and ~ 0.5 , corresponding to part of the top of the main peak and to the rise of the secondary peak, respectively. The results from our two observations show similar behavior with pulse phase of the power-law slope. Instead the N_H values as a function of pulse phase are much flatter in the August 10 observation compared with the March 17 observation.

We have also computed a modulation index, defined as

$$\Phi(E) = 1 - \frac{I_{\min}(E)}{I_{\max}(E)},$$

where I_{\max} is the maximum intensity in the background-subtracted light curve and I_{\min} is the minimum, at the given energy E . This index gives information on the dependence on energy of the process which determines the modulation (Frontera & Dal Fiume 1989). The modulation index for the first observation is almost constant with energy up to 8 keV and shows an increase in the highest energy band. Instead, in the third observation, it shows an almost linear increase with energy from 3 to 12 keV. The results are shown in Figure 11, together with the modulation indices observed by MKHN and by Clark et al. (1990). The indices from the *Tenma* and *Ginga* observations were calculated by us on the basis of the published light curves. It is apparent a similar trend to rise with energy up to 20 keV. The dependence on energy is much flatter in *Ginga* data above 20 keV. In addition, our observation of March 17 shows a different behavior: the fact that the modulation index is constant between 1 and 8 keV in the March 17 observation suggests that the dependence of this index on energy can vary with time.

3. DISCUSSION

3.1. Timing Measurements

The *EXOSAT* observations of the X-ray binary pulsar 4U 1538–52 confirm the general spin-down trend of the pulse period. Indeed, the main theoretical problem about this pulsar consists in the lack of secular spin-up. Classical theories of both disk and wind accretion predict some occasional spin-down episode but a net spin-up trend over long time scales

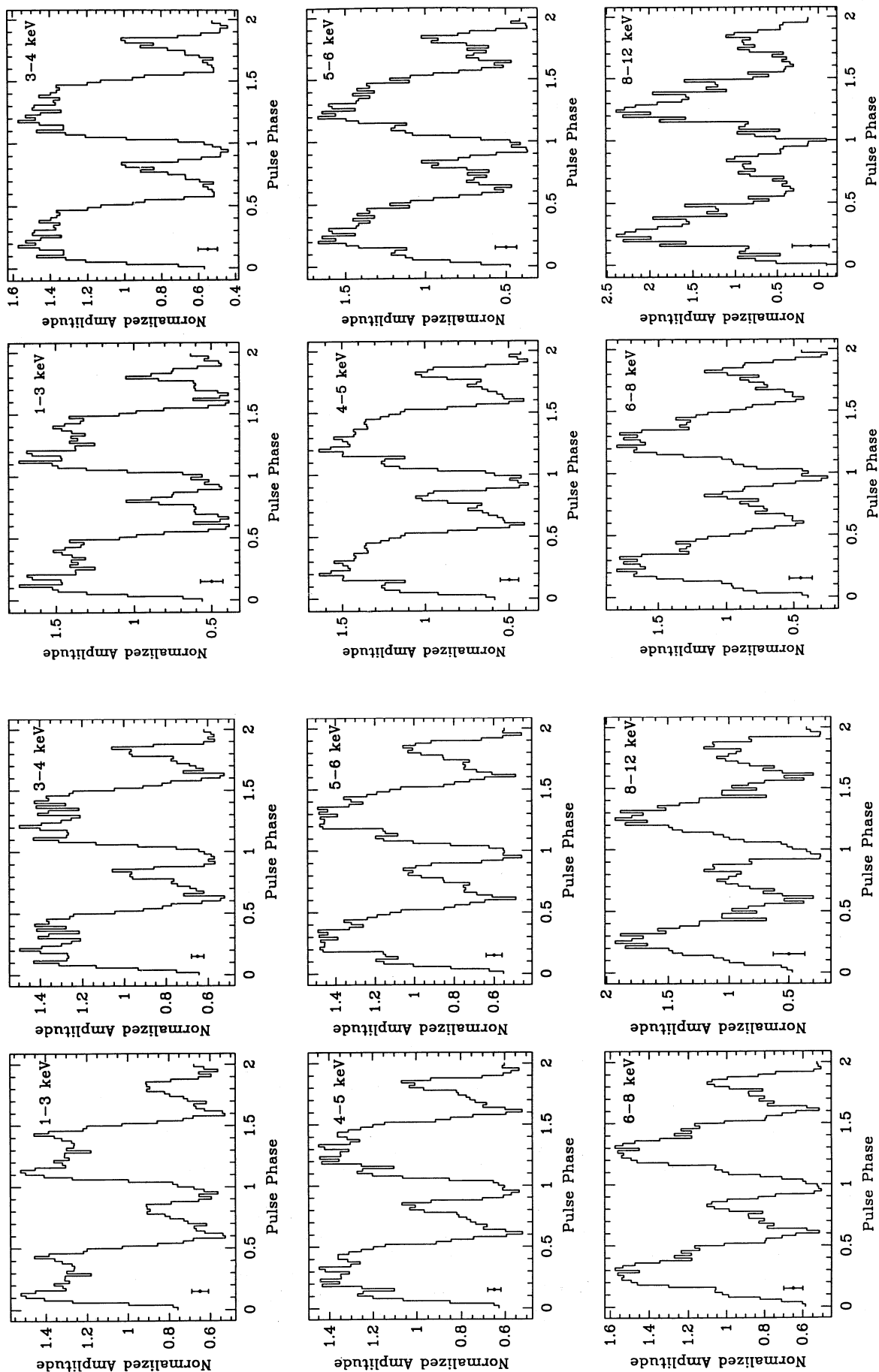


FIG. 8

FIG. 9

FIG. 8.—Folded light curves as a function of pulse phase for different energy intervals, as observed on 1984 March 17. Amplitudes are normalized to the average count rate. Background is subtracted.
 FIG. 9.—Folded light curves as a function of pulse phase for different energy intervals, as observed on 1984 August 10. Amplitudes are normalized to the average count rate. Background is subtracted.

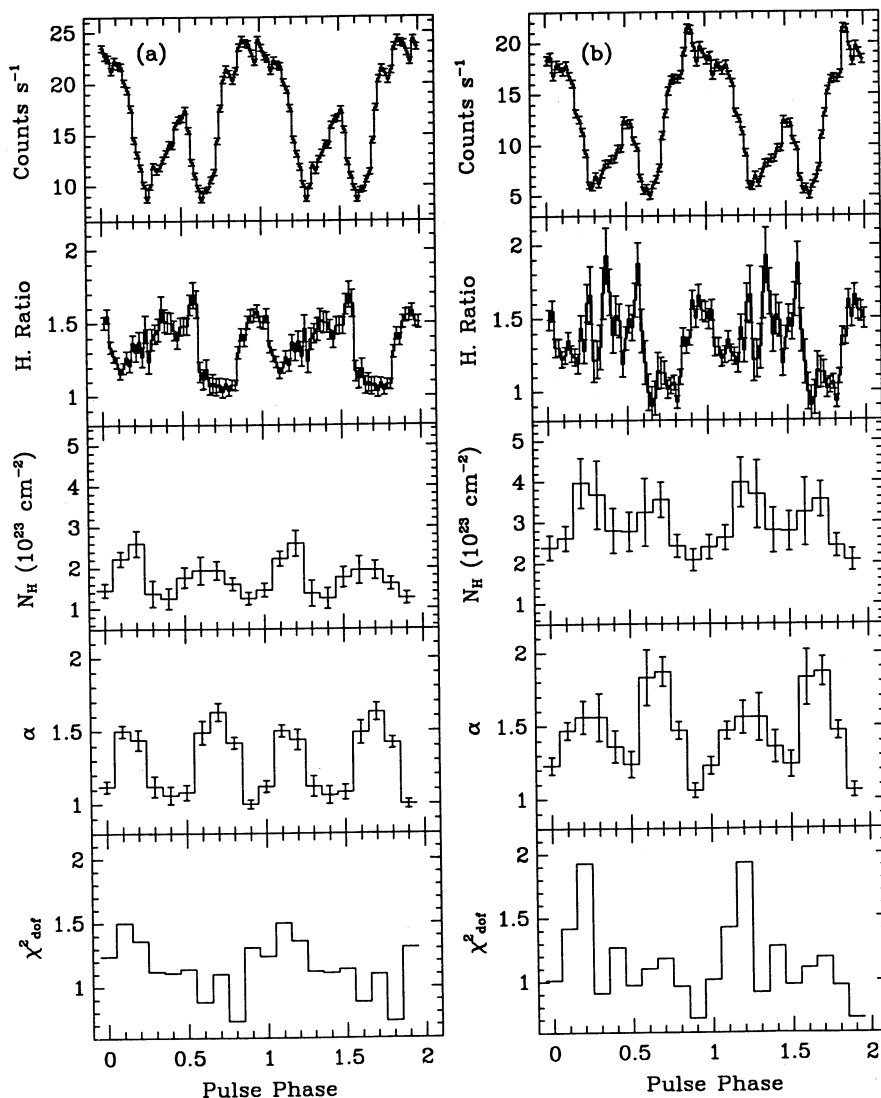


FIG. 10.—Results of the pulse-phase resolved spectroscopy for (a) day 77 and (b) day 223. From top to bottom: 1–10 keV light curve; hardness ratio (4–11 keV)/(1–4 keV) as a function of pulse phase; slope α_{ph} of the power law as a function of pulse phase; values of N_H as a function of pulse phase; values of χ^2_{dof} from the fit with power law.

(Henrichs 1983). This discrepancy was already stressed by MKHN, and our data strengthen their conclusions.

Our data also support a model in which \dot{P}_p randomly reverses sign on time scales comparable to the orbital period (Nagase et al. 1984; Boynton 1984). We repeat the calculation of MKHN based on the random walk model. MKHN measured during the observation of 1983 July an “instantaneous” spin-down rate $\dot{P}_p/P_p \sim 1.1 \times 10^{-10} \text{ s}^{-1}$. They used this value as a typical magnitude of the instantaneous rate of period change and assumed that the pulse period polarity reversed at random with a step of ~ 4 days (the binary period). During 1983–1984, using the *EXOSAT* and *Tenna* data, the spin-down rate was $\dot{P}_p/P_p \sim 1.9 \times 10^{-11} \text{ s}^{-1}$, i.e., quite higher than the 1976–1988 average ($\dot{P}_p/P_p \sim 7.3 \times 10^{-12} \text{ s}^{-1}$), and a factor only ~ 6 below the “instantaneous” spin-down rate measured by MKHN. With a typical step of $\pm 0.02 \text{ s}$ and ~ 110 steps from 1983 July to 1984 August we expect a rms period change of $(0.02)(110)^{1/2} \sim 0.21 \text{ s}$. The observed change is $\sim 0.35 \text{ s}$. This value is still consistent with the random walk model. The

inconsistency with the wind-accretion theory, that predicts a net spin-up on a long time scale, still persists.

We detected prominent aperiodic time variability from 4U 1538–52, between 0.5 and 50 mHz. This time variability does not show any characteristic time scale, but the usual power-law shape with frequency ($kf^{-\alpha}$), with a slope α , between 1 and 2, that is quite common in accreting X-ray binaries. No significant feature that could be associated to quasi-periodic oscillations is apparent in the PSDs of 4U 1538–52. In spite of that, features in the continuum power spectra of X-ray pulsars have been observed (Angelini, Stella, & Parmar 1989; Tennant 1989, cited by van der Klis 1989; Angelini, Stella, & White 1990) and the power spectra of the pulsars can be interpreted as signature of instabilities in the accretion of matter onto the polar caps. How these instabilities develop and what physical process generates them is still debated. It can be safely concluded that in any case this aperiodic variability seems to be a rule between X-ray pulsars, and in accreting sources in general. Therefore a general mechanism must act in order to produce a

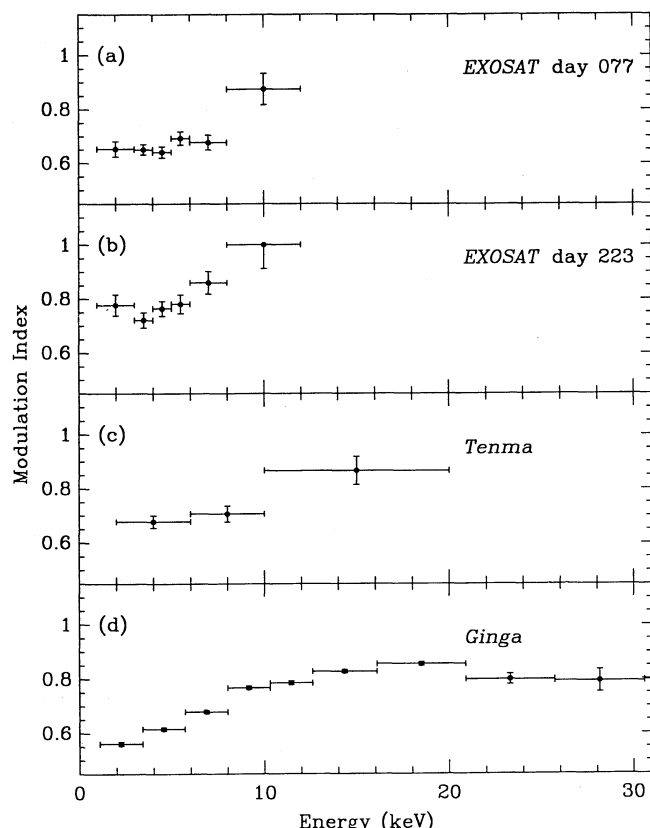


FIG. 11.—Modulation index of 4U 1538–52: (a) EXOSAT observation of March 17; (b) EXOSAT observation of August 10; (c) Tenma observation (from MKHN); (d) Ginga observation (from Clark et al. 1990).

similar kind of variability in quite different kind of sources: from cataclysmic variables to low-mass X-ray binaries to high-mass X-ray binaries.

3.2. Spectral Measurements

The analysis of energy spectra has confirmed the spectral shape, which is typical of this class of objects, while the $K\alpha$ iron emission line with an EW of 100 eV strengthens the results obtained by Tenma (MKHN). The pulse-phase-averaged hardness ratio, computed between the two energy bands 4–11 keV and 1–4 keV, does not show any correlation with the intensity of the source (see Fig. 6). Indeed, during a flaring episode, observed during the 1984 March 17 observation in which the mean intensity increases by about a factor of 2, the hardness ratio remained nearly constant. This is a confirmation of the inherently stable processes that drive the formation of X-ray spectra in X-ray pulsars (see, e.g., Dal Fiume, Frontera, & Morelli 1988), both on short and on long time scales. In fact, our measured phase-averaged energy spectra are very consistent with all previous measurements of this source.

The episode of increased absorption visible in Figure 6a can be interpreted as due to an inhomogeneity in the stellar wind of QV Nor, this being supported by the increase in the low-energy cutoff. In addition, a variation in the spectral ratio in correspondence of the iron line energy is apparent in Figure 7. A possible explanation for this evidence is that the same blob responsible for the increased absorption, obscures part of the region surrounding the pulsar that emits the iron line. The

significance of the spectral variation was tested using various spectra obtained outside this episode of increased absorption. Our spectral fits, reported in Table 3, show unambiguously that this increased hardness ratio is due to an increase in the N_H value. Unfortunately, the statistical quality of our spectra does not allow a direct estimate of the iron line intensity. In any case, the spectral ratio and the spectral fits show unambiguously that there was a simultaneous change in the N_H value and in the intensity near the iron line energy.

Our data can add some morphological detail to the description of the X-ray pulses from 4U 1538–52, but, due to the limited energy band, cannot give much improvement to our knowledge of the beaming pattern of this pulsar.

The pulse-phase resolved spectroscopy showed that the top of main peak and the rise of the secondary one have the hardest spectra. This result is in good qualitative agreement with the results obtained by Ginga (Clark et al. 1990), taking into account the uncertainty in assuming a reference point for phase 0 for different observations.

In fact, Clark et al. (1990) divide the pulse phase in eight equispaced intervals, with the lowest values of α_{ph} in bins centered at phase 0.06 and 0.44, corresponding to the top of the main peak and to the rise of the secondary one. The comparison must be made taking into account only α_{ph} , given that the energy band of EXOSAT ME is narrower than that of Ginga LAC.

Also the values of α_{ph} are in fair agreement, the Ginga data seemingly with a wider range of variation than the EXOSAT ones.

The pulse shape of 4U 1538–52 as observed by EXOSAT shows clear microstructures and a complex hardness ratio as a function of pulse phase, quite reminiscent of those observed in Vela X-1 (McClintock et al. 1976) and A0 535+26 (Bradt et al. 1976). The complexity of the hardness ratio is one of the signatures of the presence of a superstrong magnetic field, whose intensity, on the basis of the cyclotron line measured by Ginga, now we know to be $\sim 1.7 \times (1+z) \times 10^{12}$ G, where $(1+z)$ is the gravitational redshift factor (Clark et al. 1990). This complexity shows that the apparent simplicity of the two-peaked pulse profile cannot be used to model the X-ray emission from the polar caps.

A measure of the “effectiveness” of the magnetic field in the flux modulation (i.e., how sharp are the pulses), is the modulation index, reported in Figure 11. In our first observation the modulation index is almost constant from 1 to 8 keV, while in the second one it continuously increases with energy from $\sim 70\%$ in the energy interval centered at 3.5 keV up to a value near to 100% in the energy interval centered at ~ 10 keV. Ginga and Tenma data confirm that the modulation index approach 100% above 10 keV.

It is interesting to note that a suggestion was made (Kirk & Trümper 1982; Frontera et al. 1985) that the pulsed fraction and the modulation index can approach 100% in the vicinity of the cyclotron line energy. In the case of 4U 1538–52 we know that this energy is ~ 20 keV. Moreover, a suggestion was made (Frontera & Dal Fiume 1989) that there is a trend to increase with energy, with tendency to deviate from this trend in the energy interval within which a cyclotron line feature has been observed. Figure 11 shows that the modulation index seems to reach some kind of “saturation” in the vicinity of the cyclotron line energy, this being in agreement with the suggestion before mentioned.

There is evidence that the modulation index slightly changes

in different observations. On one hand, it is not surprising that the modulation index varies from observation to observation: most of X-ray pulsars show different pulse shapes in different observations. On the other hand, the variation in the modulation index is not only in its value, but also in the dependence on energy, this being a challenge to the theoretical models.

A long-term monitoring of the source can clarify the phenomenological scenario and bring better understanding of

the behavior of the modulation index and of its implications in modeling the X-ray emission from this source.

This research was supported by the Italian Space Agency (ASI) and by the Ministero della Ricerca Scientifica e Tecnologica (MURST). We thank L. Nicastro, who developed the FORTRAN code to fit the Power Spectral Densities and gave assistance for the fits.

REFERENCES

- Angelini, L., Stella, L., & Parmar, A. N. 1989, *ApJ*, 346, 911
 Angelini, L., Stella, L., & White, N. E. 1991, *ApJ*, 371, 332
 Apparaio, K. M. V., Bradt, H. V., Dower, R. G., Doxsey, R. E., Jernigan, J. G., & Li, F. 1978, *Nature*, 271, 225
 Becker, R. H., Swank, J. H., Boldt, E. A., Holt, S. S., Pravdo, S. H., Saba, J. R., & Serlemitsos, P. J. 1977, *ApJ*, 216, L11
 Belloni, T., & Hasinger, G. 1990, *A&A*, 230, 103
 Boynton, E. P., Deeter, J. E., Lamb, F. K., Zylstra, G., Pravdo, S. H., White, N. E., Wood, K. S., & Yentis, D. J. 1984, *ApJ*, 283, L53
 Bradt, H., et al. 1976, *ApJ*, 204, L67
 Clark, G. W., Woo, J., Nagase, F., Makishima, K., & Sakao, T. 1990, *ApJ*, 353, 274
 Cowley, A. P., Crampton, D., Hutchings, J. B., Liller, W., & Sanduleak, N. 1977, *ApJ*, 218, L3
 Crampton, D., Hutchings, J. B., & Cowley, A. P. 1978, *ApJ*, 225, L63
 Dal Fiume, D., Frontera, F., & Morelli, E. 1988, *ApJ*, 331, 313
 Davison, P. J. N. 1977, *MNRAS*, 179, 35P
 Davison, P. J. N., Watson, M. G., & Pye, J. P. 1977, *MNRAS*, 181, 73P
 de Korte, P. A. J., et al. 1981, *Space Sci. Rev.*, 30, 495
 Forman, W., Jones, C., Cominsky, L., Julien, P., Murray, S., Peters, G., Tananbaum, H., & Giacconi, R. 1978, *ApJS*, 38, 357
 Frontera, F., & Dal Fiume, D. 1989, in *Proc 23d ESLAB Symp., X-Ray Binaries*, ed. J. Hunt & B. Battick, ESA SP-296 (Noordwijk: ESA) 57
 Frontera, F., Dal Fiume, D., Morelli, E., & Spada, G. 1985, *ApJ*, 298, 585
 Henrichs, H. F. 1983, in *Accretion-driven Stellar X-Ray Sources*, ed. W. H. G. Lewin & E. P. J. Van den Heuvel (Cambridge Univ. Press), 393
 Kirk, J. G., & Trümper, J. 1982, in *Accretion-driven Stellar X-Ray Sources*, ed. W. H. G. Lewin (Cambridge Univ. Press), 261
 Koyama, K. 1989, *PASJ*, 41, 665
 Lewin, W. H. G., van Paradijs, J., & van der Klis, M. 1988, *Space Sci. Rev.*, 46, 273
 Makishima, K., Koyama, K., Hayakawa, S., & Nagase, F. 1987, *ApJ*, 314, 619 (MKHN)
 McClintock, J. E., et al. 1976, *ApJ*, 206, L99
 Nagase, F. 1989, *PASJ*, 41, 1
 Nagase, F., et al. 1984, *PASJ*, 36, 667
 Nagase, F., Hayakawa, S., Sato, N., Masai, K., & Inoue, H. 1986, *PASJ*, 38, 547
 Parkes, G. E., Murdin, P. G., & Mason, K. O. 1978, *MNRAS*, 184, 73P
 Schwartz, D. A., Gursky, H., Schwartz, J., Bradt, H., & Doxsey, R. 1978, *Nature*, 275, 517
 Taylor, B. G., Andresen, R. D., Peacock, A., & Zobl, R. 1981, *Space Sci. Rev.*, 30, 479
 Turner, M. J. L., Smith, A., & Zimmermann, H. U. 1981, *Space Sci. Rev.*, 30, 513
 van der Klis, M. 1989, *ARA&A*, 27, 517
 Warwick, R. S., Turner, M. J. L., Watson, M. G., & Willingale, R. 1985, *Nature*, 317, 218
 White, N. E., & Peacock, A. 1988, in *X-Ray Astronomy with EXOSAT*, ed. R. Pallavicini & N. E. White (Firenze: Soc. Astron. Ital.), 7
 White, N. E., Swank, J. H., & Holt, S. S. 1983, *ApJ*, 270, 711